Transparent wood for functional and structural applications
Author(s): Yuanyuan Li, Qiliang Fu, Xuan Yang and Lars Berglund
Source: *Philosophical Transactions: Mathematical, Physical and Engineering Sciences*, Vol. 376, No. 2112, Discussion meeting issue: New horizons for cellulose nanotechnology (13 February 2018), pp. 1-15
Published by: Royal Society
Stable URL: https://www.jstor.org/stable/44678872
Accessed: 22-02-2022 08:55 UTC

PHILOSOPHICAL TRANSACTIONS A

rsta.royalsocietypublishing.org

Review

Cite this article: Li Y, Fu Q, Yang X, Berglund L. 2018 Transparent wood for functional and structural applications. *Phil. Trans. R. Soc. A* **376**: 20170182.
http://dx.doi.org/10.1098/rsta.2017.0182

Accepted: 24 August 2017

One contribution of 14 to a discussion meeting issue 'New horizons for cellulose nanotechnology'.

Subject Areas:
materials science, energy, chemical engineering, nanotechnology

Keywords:
transparent wood, optical performance, mechanical performance, functionalization and application

Author for correspondence:
Lars Berglund
e-mail: blund@kth.se

Transparent wood for functional and structural applications

Yuanyuan Li, Qiliang Fu, Xuan Yang and Lars Berglund

Wallenberg Wood Science Center, Department of Fiber and Polymer Technology, KTH Royal Institute of Technology, 10044 Stockholm, Sweden

YL, 0000-0002-1591-5815

Optically transparent wood combines mechanical performance with optical functionalities is an emerging candidate for applications in smart buildings and structural optics and photonics. The present review summarizes transparent wood preparation methods, optical and mechanical performance, and functionalization routes, and discusses potential applications. The various challenges are discussed for the purpose of improved performance, scaled-up production and realization of advanced applications.

This article is part of a discussion meeting issue 'New horizons for cellulose nanotechnology'.

1. Introduction

Cellulose-based biocomposites are of interest as semi-structural and eco-friendly materials due to the desire to reduce our dependence on synthetic polymers [1]. Low density, favourable mechanical properties, renewable resource origin and low cost are important drivers for using biocomposties in applications ranging from automotive composites to electronic devices [2–5].

Wood derives its mechanical performance primarily from the cellulose component, and is the most widely used bio-based structural material. Wood shows several levels of hierarchical structure [6], and has a characteristic anisotropic organization with open channels for liquid transport [7]. The porous structure is of great complexity combing micro-, meso- and macro-pores [8]. The nanoscale organization of the cell wall as a nanoporous cellulose fibril composite provides opportunity for tailored design of advanced wood-based multi-functional materials with preserved structural performance [9].

THE ROYAL SOCIETY PUBLISHING

Native wood is obviously non-transparent, and this offers an interesting materials science challenge.

Cellulose fibres extracted from wood in the form of pulp fibres have been intensively studied to make transparent paper and films [5]. Wood chips at centimetre scale are subjected to 'cooking'. The lignin-rich region in the middle lamella and cell wall corner are degraded, so that individual wood tracheid cells in the form of fibres become liberated. These chemical pulp fibres are mainly composed of nanoscale cellulose fibrils and amorphous hemicellulose, and can be used to prepare transparent paper or transparent films. Preparation strategies include cellulose dissolution and regeneration [10], impregnation of porous paper with a polymer [11,12] or decreasing the diameter of the cellulose fibrils to the nanoscale [2,13]. However, the final materials are hard to compete with the original wood tissues in terms of hierarchical structure and oriented cell structure, which may limit their applications where more complex structure is needed. In terms of designing materials based on biological tissues with preserved structure, the generality of the approach was illustrated by Shams *et al.*, who prepared a transparent crab shell [14]. Calcium carbonate and proteins were removed, and the nanoporous chitin fibril network was impregnated with a polymer having similar refractive index as chitin.

Transparent wood was first prepared with preserved structure, for the purpose of wood morphology studies [15]. Li *et al.* then reported physical properties of transparent wood and pointed out the potential for engineering applications [16]. After this, several publications have discussed various potential applications in smart buildings and structural optics and photonics [15–23]. The present review summarizes recent progress and challenges for transparent wood preparation, improved optical and mechanical performance, new functionalization approaches and applications.

2. Basics of light–wood interaction

When light travels through air and interacts with a solid object, light propagation may continue in the forward direction for refraction and/or absorption, or it may be reflected backwards at the air/solid interface, figure 1*a*). Some terms are of importance during discussions of optical properties of a transparent material [25]. The total optical transmittance (here we use transmittance for short) of an object is the ratio of transmitted light intensity (both directly transmitted $I_{T,direct}$ and diffused transmitted $I_{T,diffuse}$) to the incident light intensity I_{I0}. The total transmittance is then $(I_{T,direct} + I_{T,diffus})/I_{I0}$. The optical haze is the ratio of diffused transmitted light $I_{T,diffus}$ to the total transmitted light, $I_{T,diffus}/(I_{T,direct} + I_{T,diffus})$ depicted in figure 1*a*. Light is refracted as it transmits through an object due to the difference in the refractive index, and the refraction angle obeys Snell's law, $n_1 \sin\theta_1 = n_2 \sin\theta_2$ [26]. Several parameters may influence the optical transmittance and haze of an object, including the refractive index, thickness, surface roughness, porosity, pore size distribution, etc. [27–29]. For the case of two-phase materials such as microscale composites, the higher the refractive index contrasts between the two media, the stronger the scattering of light. As a result, a larger percentage of light is reflected, leading to lower transmittance. Light attenuation (I_A in figure 1*a*) takes place by transferring light to other types of energy, such as heat. With larger thickness or a larger number of solid–solid interfaces in the composite, more light attenuation takes place, and transmittance is lowered. The Beer–Lambert law could be employed to explain this phenomenon [30]. In order to make a composite material transparent, low refractive index contrast between phases and low light attenuation are needed. Obviously, lower thickness results in higher transmittance. It should also be mentioned that for nanocomposites, the small scale of the phase domains makes refractive index differences less critical.

Wood is a non-transparent material due to its optical heterogeneous nature, including microscale porous structure, different chemical components in the cell wall with different refractive indices and the presence of strongly light-absorbing chemical entities. Figure 1*b* is a micrograph of the softwood structure, showing the aligned hollow fibre cells. When light interacts with wood, a combination of reflection, refraction, absorption and transmission occurs. Light

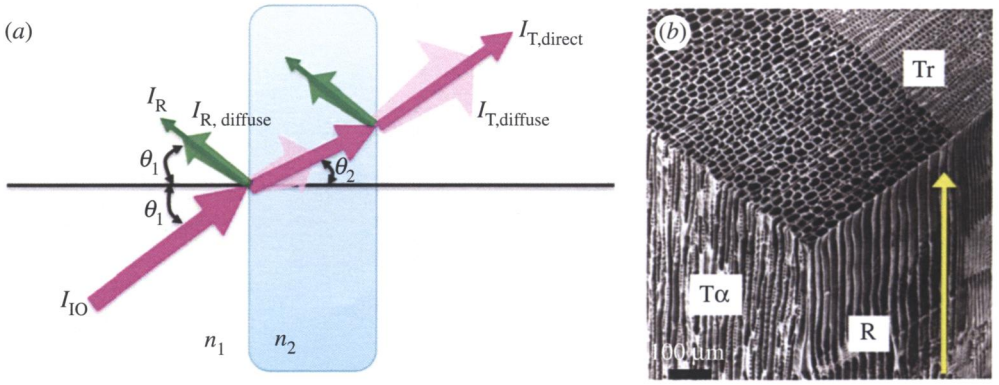

Figure 1. (*a*) Sketch illustrating light propagation through a solid object (blue) in a medium (i.e. air), where I_{IO}, incident light intensity; $I_{T,directe}$, intensity of directly transmitted light; $I_{T,diffuse}$, intensity of diffusely transmitted light; I_R, intensity of reflected light; $I_{R,diffuse}$, intensity of diffusely reflected light; θ_1, incident angle; θ_2, refracted angle, n_1 and n_2 represent the refractive indices of the medium and the solid object. (*b*) Typical SEM image of wood structure (softwood), showing the aligned porous structure with 'pipe-like' wood tracheid fibre cells. Note the abrupt transition between low-density earlywood and higher density latewood regions. Tr, transverse plane; Tα, tangential plane; R, radial plane. The yellow arrow represents the longitudinal direction. Scale bar is 100 µm [24].

scattering takes place at all interfaces between the cell wall (refractive index around 1.56) and air (refractive index of 1.0). Inside the cell wall, mismatch of refractive index of the main chemical components of cellulose (1.53), hemicellulose (1.53) and lignin (1.61) is likely to lead to light scattering [15]. In addition, strong light absorption takes place in wood due to the existence of light-absorbing components in the cell wall, among which lignin accounts for 80–95% of the light absorption [31]. The interaction details depend on the wavelength of the light and the nature of the wood such as density, chemical compositions, wood directions etc. Generally, in order to make wood transparent, light absorption from chemical entities need to be reduced or eliminated. Light scattering at the air/cell wall interfaces and inside the cell walls should be minimized.

3. Transparent wood fabrication

The current preparation approach is mainly based on delignification of the substrate followed by infiltration of a polymer with refractive index matching the wood substrate (figure 2) [16–18]. Delignification decreases light absorption in wood, and the refractive index mismatch in the cell wall. Fink treated wood with a 5% aqueous solution of sodium hypochlorite (recorded as NaClO method) for 1–2 days to remove coloured substances, including lignin [15]. Yano [32] reported lignin removal from wood through sodium chlorite treatment at 45°C for 10 h. Berglund's group obtained delignified wood through modified sodium chlorite method at 80°C for 6 h (recorded as $NaClO_2$ method). The lignin content was strongly decreased from around 25% to less than 3% [17]. Other researchers have also adapted the $NaClO_2$ method [21,22,33]. Hu's group removed lignin by cooking in NaOH and Na_2SO_3 solution, followed by hydrogen peroxide (H_2O_2) treatment, resulting in a lignin content lower than 3% (recorded as $NaOH/Na_2SO_3 + H_2O_2$ method) [34]. Yu *et al.* [20] also used this method. After delignification processes, the wood colour changes from brownish to white, as shown in figure 2. Berglund's group characterized the change in wood structure upon delignification. The honeycomb-like structure was preserved compared with the original wood (figure 3*a*,*b*). The presence of micro-scale and nano-scale voids in the cell wall was attributed to the removal of lignin (figure 3*a*,*b*), leading to increased specific surface area. The specific surface areas increase from 1.2 $m^2\,g^{-1}$ for the original wood to 20 $m^2\,g^{-1}$ for the delignified wood template (figure 3*c*) [17]. Preservation of the anisotropic wood structure and increased nanoscale pores was supported by results

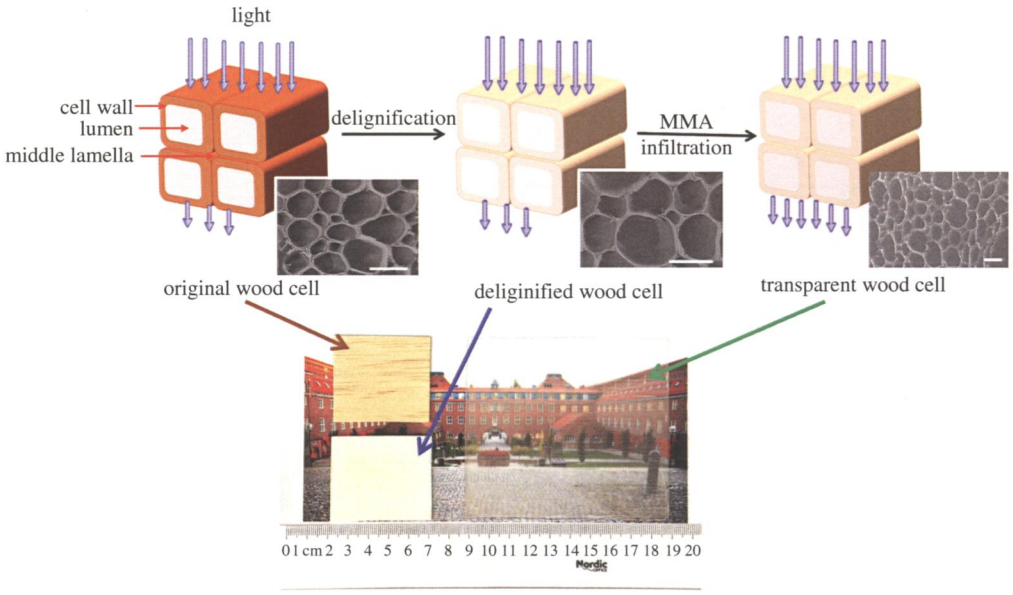

Figure 2. Sketch showing transparent wood preparation: delignification followed by polymer infiltration. Scale bars in the SEM images are 40 µm. Reproduced with permission from Li *et al.* [17] (Copyright © 2016 American Chemical Society).

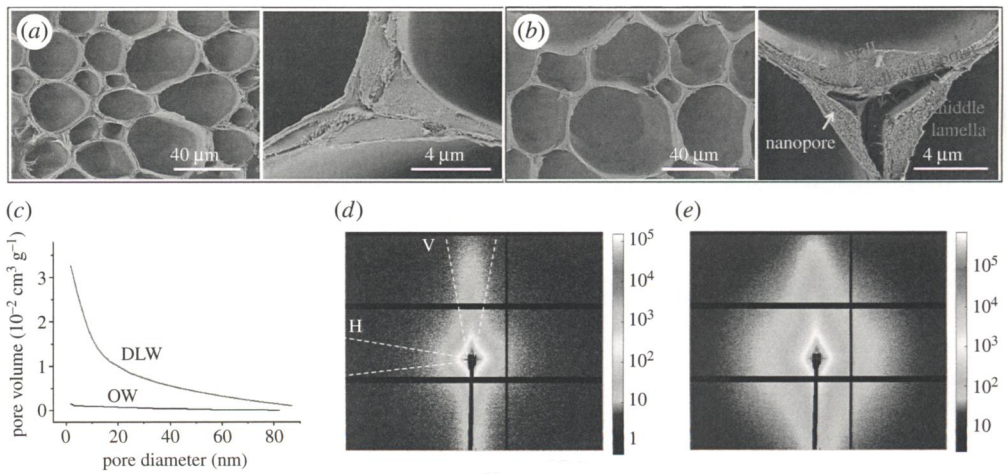

Figure 3. (*a*) Images of original wood cross-section showing the cellular structure of wood. (*b*) Images of delignified wood supporting the presence of a well-preserved wood structure, and the generation of micro-scale and nano-scale voids in the cell wall. (*c*) Pore size distribution from BET desorption analysis of original wood and delignified wood confirming generation of nanopores due to delignification. Two-dimensional SAXS patterns of original wood (*d*) and delignified wood (*e*) [17]. Reproduced with permission from Li *et al.* [17] (Copyright © 2016 American Chemical Society). (Online version in colour.)

from small-angle X-ray scattering, [17,35,36] as shown in figure 3*d*,*e*. The two-dimensional small-angle X-ray scattering data from original wood and delignified wood both show twofold symmetry anisotropic intensity distribution with a strong streak, indicating the preservation of the anisotropic wood structure. The increased intensity for the delignified wood was confirmed due to the increased pore density by lignin removal. The present authors demonstrated that delignification is not a necessary step for transparent wood preparation [37]. Compared with

the delignification alternative, wood template with the same whiteness was obtained by only removing components containing chromophoric structures. Up to 80% of lignin was retained with better-preserved wood structure and higher mechanical strength. The procedure was demonstrated to be more efficient and environmentally benign.

Polymer infiltration of the porous template was then carried out in order to reduce the refractive index contrast and obtain high optical transmittance. Proper selection of transparent polymers with refractive indices matching the cell wall is needed. The refractive index of wood tissue may vary depending on the wood species, delignification efficiency, etc., as pointed out by Fink [15]. The polymers applied to make transparent wood are listed here with refractive index in the bracket: poly(methyl methacrylate) (PMMA, approx. 1.49), epoxy resin (approx. 1.5), polyvinylpyrrolidone (PVP, 1.53), *n*-butyl methacrylate (1.50), polystyrene (1.59), dibutyl phthalate (1.52), iso-bornyl methacrylate (1.48–1.50), diallyl phthalate and poly vinylcarbazole (1.68) [15–22,34]. Different polymers demonstrate different viscosity, refractive indices and shrinkage properties, which influences the transparent wood preparation and properties. Fink tried with polymer mixtures to minimize the refractive index contrast between wood and infiltrating polymer, and decrease the viscosity and shrinkage of the polymer [15]. After polymerization, transparent wood with an optical transmittance exceeding 80% and haze over 75% can be obtained. The information about transparent wood with various infiltration polymers is summarized in table 1 and in the following text.

Despite the success in transparent wood fabrication, challenges exist in order to improve optical and mechanical properties and scale-up the production methods. From the point of rational preparation, the delignification processes are time-consuming and not always eco-friendly. In addition, removal of lignin will weaken the wood structure, so that handling and fabrication of large substrates becomes challenging. Removing only chromophore works for transparent wood preparation; however, the optical performance stability is a potential question for real applications. Polymer properties are important for transparent wood fabrication and performance. Important parameters are refractive index, viscosity, compatibility with cell wall, shrinkage during polymerization, etc. Thus, polymer selection is vital. Furthermore, transparent wood with increased cellulose content is desirable. This can be achieved by compressing the wood structure, although it is dubious if this is feasible for thick structures.

4. Transparent wood optical properties

The current reported transparent wood demonstrates good optical transmittance and high haze (table 1). When light interacts with transparent wood, the following three interactions are considered.

(i) Reflection at outer gas/transparent wood interface: Transparent wood shows high transmittance and high optical haze, with minor reflection at the outer surface. Li *et al.* [16] reported about 10% of reflection for transparent wood with thickness in the longitudinal direction.

(ii) Scattering in the form of refraction and reflection: In transparent wood, light scattering mainly happens at the interface between wood tissue and polymer. The polymers with different refractive indices used for transparent wood preparation are summarized in table 1. The lower the refractive index contrast between the wood template and the polymer, the less scattering will take place at the interfaces. It should be mentioned that with nanoscale phase domain size, the refractive index matching does not need to be as good as is required for micro-scale domain size [38]. The high haze is primarily due to collective scattering inside the composite material. The increased light scattering is apparent when a laser beam is transmitted through wood [17,18]. It is also a challenge to obtain perfect interfaces between the polymer and the wood tissue, because there is substantial risk for interfacial gaps between the polymer in the lumen and the wood cell

Table 1. Summary of transparent wood preparation and properties. The optical properties are values at the wavelength of 550 nm. T, transverse plane; L, longitudinal direction; *t*, thickness; Tr, transmittance; *E*, elastic modulus; σ, tensile strength; ε, strain to failure. All the transparent wood directions are remarked according to our method mentioned above. Mechanical properties from [22] are the data from luminescent transparent wood.

					optical property			mechanical performance			
	wood species	template preparation method; temperature; time	polymer	wood thickness direction	*t* (mm)	Tr (%)	haze (%)	$l \times w \times t$ (mm^3)	*E* (GPa)	σ (MPa)	ε (%)
Li *et al.* [17]	balsa	$NaClO_2$; 80°C; 6 h	PMMA	T	0.7	90	approximately 50	60 × 5 × 1.2	3.59	90	approximately 3.5
					3.7	40	approximately 80				
Gan *et al.* [21]	cathay poplar	$NaClO_2$; 80°C; 12 h + H_2O_2; boiling;4 h	PMMA	—	0.5	86.1	—	50 × 10 × 3	2.66	45.92	approximately 5.5
Yu *et al.* [38]	beech	NaOH/Na_2SO_3; boiling; 48 h + H_2O_2	PMMA	T	5	86	90	60 × 30 × 5	2.67	60.1	approximately 4.8
Yaddanapudi *et al.* [34]	beech	$NaClO_2$; 95°C; 12 h	PMMA (RI = 1.49)	—	0.1	70	—	50 × 3 × ?	2.5	150	approximately 10
					0.3	30	18				
					0.6	15	40				
					0.7	10	49				
Zhu *et al.* [18]	bass	NaOH/Na_2SO_3; boiling; 7 h + H_2O_2; boiling; 5 h	epoxy (RI = approx. 1.5)	L	2	90	approximately 95	50 × 10 × 3	1.22	23.38	approximately 4

(*Continued*.)

Table 1. (*Continued.*)

	wood species	template preparation method; temperature; time	polymer	wood thickness direction	optical property			mechanical performance			
					t (mm)	Tr (%)	haze (%)	$l \times w \times t$ (mm^3)	E (GPa)	σ (MPa)	ε (%)
		$NaOH/Na_2SO_3$; boiling; 3 h + H_2O_2; boiling; 3 h		T		approximately 80	approximately 85	50 × 10 × 3	2.37	45.38	approximately 4.3
Zhu *et al.* [19]	bass	$NaOH/Na_2SO_3$; boiling; 12 h + H_2O_2; boiling	PVP (RI = 1.53)	L	1	90	80	50 × 10 × 3	—	11.7	6
Li *et al.* [16]	bass	$NaOH/Na_2SO_3$; boiling; 3 h + H_2O_2; boiling; 2–3 h	epoxy (RI = approximately 1.5)	L	5	90	95	—	—	—	—
Fink [15]	broad leaved lime, field elm, ash and champion oak	NaClO; 24–48 h	mixture A[a] (RI = 1.55–1.57)	T	up to 4	—	—	—	—	—	—
			mixture B[b] (RI = 1.56)								

[a]Polymers: butyl methacrylate, styrene and dibutyl phthalate.

[b]Polymers: iso-bornyl methacrylate, diallyl phthalate and vinyl carbazole.

wall. There are two main reasons: (i) the compatibility between the polymer and the wood template may not be sufficient, and (ii) the polymer will shrink during polymerization.

(iii) Absorption inside transparent wood: Light absorption is mainly due to the presence of lignin in wood. Delignification and lignin modification were applied by removing components containing chromophores to minimize light absorption. Detailed information is presented in the transparent wood preparation section.

There is interest in considering the effects of material parameters, including wood specimen thickness and cellulose volume fraction on the transparent wood optical properties. As wood thickness increases, the transmittance will decrease and haze will increase. This is caused by the increasing amount of light attenuation with longer light pathway, and the increasing number of polymer/wood interfaces leading to light scattering. Li *et al.* [17] reported that as the thickness of transparent wood increased from 0.7 to 3.7 mm, the transmittance decreased from 90 to 40%, and the haze increased from 50 to 80% (figure 4*a*). The cellulose volume fraction is another important parameter. Transparent wood with different cellulose volume fractions but the same thickness can be obtained by compressing wood template before polymer impregnation. Figure 4*b* shows that the transmittance will decrease and haze will increase, primarily due to the larger number of wood/polymer interfaces [17]. Light scattering of transparent wood based on different wood species may vary substantially due to differences in cellulose volume fraction and cellular morphology.

Optical anisotropy is also of interest. Wood is a highly anisotropic structured material, leading to directional-dependent optical properties. The interface density (number of interfaces per length) is higher when light propagates perpendicular to wood longitudinal direction (or propagates in the transverse plane) compared with propagates along the longitudinal direction. In this paper, transparent wood is termed L-wood when light propagates along the longitudinal and termed T-wood when light propagates in the transverse plane (or perpendicular to wood longitudinal direction). L-wood presents higher transmittance and lower haze than T-wood. This is because L-wood has a lower density of polymer/cellulose interfaces due to the hollow cylinder shape of wood cells (figure 4*c*) [18]. The light scattering pattern is also influenced by anisotropy. Most of the scattering takes place at the interface between the wood cell wall and the polymer present in the lumen. This interface is located in a more favourable position in the L-wood than in T-wood. Figure 4*d* illustrates this, in that the scattering is isotropic for L-wood, whereas the scattering effect is highly anisotropic for T-wood. In L-wood, the fibre orientation is parallel to the light direction (*z* direction), thus the scattering light exhibits a Gaussian-like distribution with similar angular distribution in both the x and y directions [18]. By contrast, the wood fibre in T-wood is aligned in the x direction, influencing scattering in the y direction. Thus, an extremely large scattering angle is observed in the y direction.

5. Transparent wood mechanical properties

The mechanical properties are important for many applications considered. They strongly depend on the wood species (including density, cellulose content, cell structure morphology, annual ring structure etc.), and wood structure anisotropy. From the results in table 1, properties of transparent wood based on balsa, poplar and beech impregnated with the same polymer show substantial differences.

Mechanical property synergies between wood and the polymer are observed for transparent wood tested along the fibre direction (figure 5*a*) [17,20]. The major load-bearing component in wood is the cellulose nanofibres. They are favourably oriented and can show favourable interaction (bonding) with PMMA (figure 5*b*,*c*). Li *et al.* [17] reported that the tensile properties of transparent wood ($V_f = 19\%$, $E = 3.59$ GPa and $\sigma = 90$ MPa) are much higher than for both the delignified wood template ($E = 0.22$ GPa and $\sigma = 3$ MPa) and for PMMA ($E = 1.8$ GPa and $\sigma = 44$ MPa). Yu *et al.* [20] observed similar results. Li *et al.* [17] reported that the tensile properties of transparent wood were improved with increased cellulose volume fraction, and the tensile

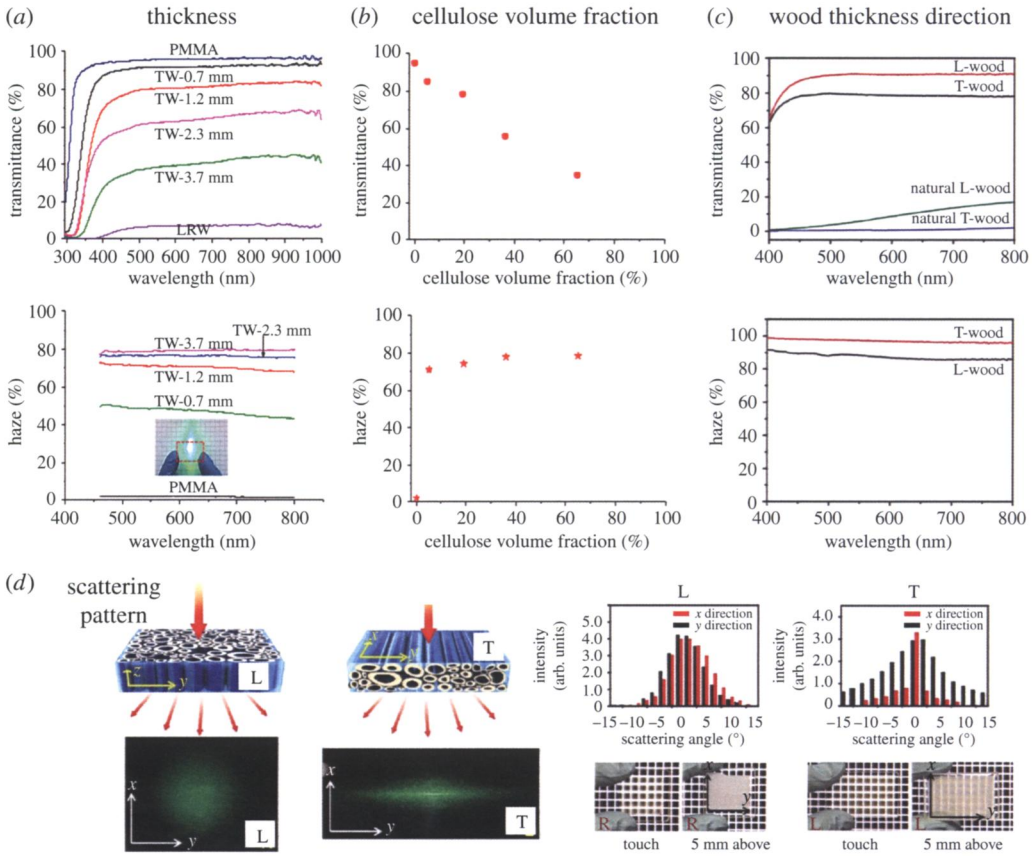

Figure 4. Transmittance and haze data for transparent wood as they vary with (*a*) thickness [17], (*b*) cellulose volume fraction [17], (*c*) wood thickness direction (anisotropy) [18] and (*d*) scattering pattern of transparent wood with different wood thickness direction (anisotropy effects) [18]. Reproduced with permission from Li *et al.* [17] (Copyright © 2016 American Chemical Society) and Zhu *et al.* [18] (Copyright © 2016 Wiley).

properties can thus be tailored by compression of the wood template to the desired thickness and cellulose content. Wood is an anisotropic material with higher modulus and strength in the longitudinal direction than in the radial direction [39]. The reason is anisotropic cell wall properties and the geometrical shape of wood fibres. The tensile properties of transparent wood are thus also anisotropic. Zhu *et al.* [18] reported the mechanical performances of transparent wood along the longitudinal direction are around double that of transparent wood perpendicular to the longitudinal direction.

One advantage of transparent wood for structural applications is that the fracture toughness is higher than for brittle materials such as glass, so that transparent wood does not shatter in an unfavourable manner [37]. Li *et al.* [16] reported the impact strength of transparent wood (figure 5*d*), and noted favourable impact toughness. This shows that transparent wood could potentially be used in applications where impact properties are important.

Incorporation of functional particles into transparent wood introduces multi-functionalities and brings new application directions. The influence of incorporating functional particles on the mechanical properties is also studied. Yu *et al.* reported that incorporation of functionalized nanoparticles (Cs_xWO_3) could decrease the mechanical properties of transparent wood. A higher content of inorganic particles resulted in reduced strength properties [20,21]. Gan *et al.* [21] obtained a similar conclusion when magnetic particles (Fe_3O_4) were introduced.

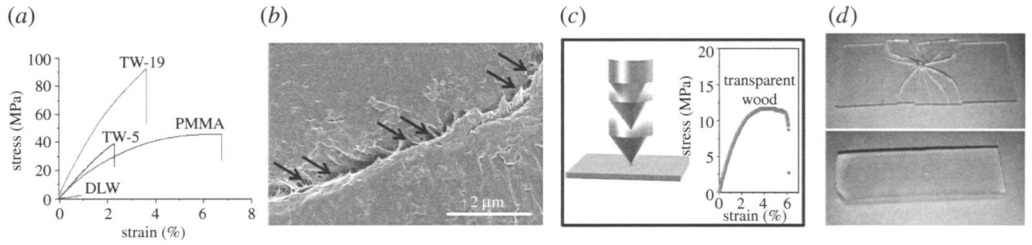

Figure 5. (*a*) Stress–strain curves in uniaxial tension for transparent wood, V_f 0.19 (TW-19) and V_f 0.05 (TW-5), delignified wood (DLW) and PMMA [17]. (*b*) SEM micrograph of transparent wood showing the nanofibrous nature of the cell wall region and signs of favourable interfacial bonding with PMMA at the PMMA/wood interface [17]. (*c*) Impact response of transparent wood, sketch (left) and stress–strain curve (right) [16]. (*d*) Comparison of glass (upper) and transparent wood (bottom) after impact test [16]. Reproduced with permission from Li *et al.* [17] (Copyright © 2016 American Chemical Society) and Li *et al.* [16] (Copyright © 2016 Wiley). (Online version in colour.)

6. Functionalization

Wood shows great potential for multi-functionalities due to the presence of multi-scale pores (from macro-scale lumen channels to nano-scale pores in cell wall), and the compositions of cellulose, hemicellulose and lignin. The main strategies are cell wall modification, cell-wall/lumen interface modification and lumen filling. Involved processes include chemical reactions, physical adsorption or absorption, thermal treatment for phase separation effects, inorganic or metal particle precipitation from salt solution, and combined approaches [9]. Successful examples include magnetic wood [40,41], UV-stabilized wood [42,43], stimuli responsive wood [37] and conductive wood [44–46]. Some technologies can potentially be used to prepare functional wood with optical transparency.

A wood template for transparent wood demonstrates higher porosity compared with the original wood [17]. The pore space is substantial and there are many possibilities to modify the template by adding functional components to the porous regions. One approach for transparent wood modification is to fill the microscale pore space (i.e. lumen space) with polymer liquids (solutions or suspensions) decorated with functional nanoparticles, followed by polymerization/curing [20–23]. Li *et al.* [23] prepared luminescent transparent wood by impregnation of silicon or CdSe quantum dots (QDs) dispersed in a PMMA monomer/oligomer liquid mixture, and the liquid was then polymerized. The approach is presented in figure 6*a*. Photoluminescence mapping revealed a uniform distribution of emission centres (figure 6*b*) with the signal intensity variation less than 10% across the image. The emission and absorption spectra of the QD-modified wood are also provided (figure 6*c*) because this confirms the successful shift in wavelengths. The quantum yield was 36%, and this as well as observed spectra are similar to that for the liquid suspension of QD. It is therefore concluded that the QDs are well dispersed in lumen space. A later study of luminescent transparent wood incorporated γ-Fe_2O_3@$YVO_4:Eu^{3+}$ nanoparticles using the same method [21]. Heat-shielding transparent wood [20] was reported by Yu *et al.*, who used Cs_xWO_3 nanoparticles with near-infrared (NIR) absorption properties. The preparation procedure was similar to that in the previous study. Light transmittance curves are presented in figure 6*d*. With increasing content of nanoparticles, the absorption in the NIR range increases, so that optical transmittance is reduced. The same trend was observed for magnetic transparent wood. Gan *et al.* [21,22] prepared magnetic wood using dispersed Fe_3O_4 and γ-Fe_2O_3@$YVO_4:Eu^{3+}$ magnetic particles. SEM and corresponding element mapping, FTIR and X-ray diffraction data confirm the presence of magnetic particles. The saturation magnetization of the transparent magnetic wood increased as the magnetic particles loading increased.

Another modification approach is to firstly modify the wood template followed by monomer impregnation and polymerization. Li *et al.* prepared luminescent wood where lasing emission

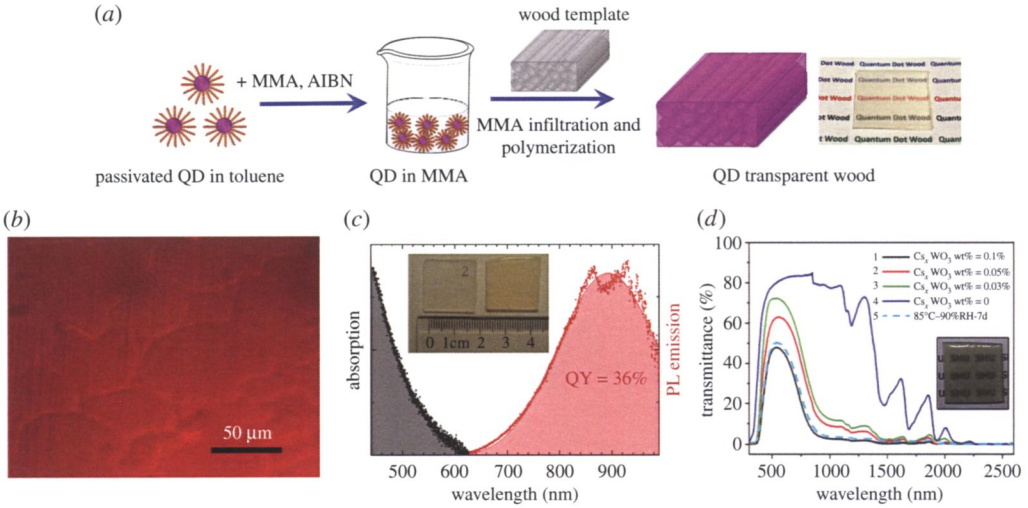

Figure 6. (*a*) Sketch of transparent wood modification procedure using QDs in order to achieve luminescence effects [23]. (*b*) Real colour photoluminescence mapping of Si QDs in transparent wood [23]. (*c*) Absorption and photoluminescent (PL) emission curves of Si QD wood. Inset image shows the actual samples: (left) transparent wood and (right) Si QD wood prepared for quantum yield (QY) measurements [23]. (*d*) Transmittance spectra of $C_{sx}WO3$/transparent wood [20]. Reproduced with permission from Li *et al.* [23] (Copyright © 2017 American Chemical Society) and Yu *et al.* [20] (Copyright © 2017 Royal Society of Chemistry).

was observed after impregnation of an organic dye (Rh6G) solution in the wood template. This was then followed by MMA monomer/oligomer impregnation and polymerization [47]. A microscopy image of the specimen and the optical transmission curve are presented to confirm the presence of the dye. Under favourable pump light conditions, cellulose fibres operate as small optical resonators and lead to lasing action so that a wood laser is created by utilization of the microstructural anisotropy in wood. As reported, the nanoparticle or molecular dye content is low (less than 1 wt%). Higher content would strongly reduce optical transmittance. It is a major challenge to increase the content of active component, and yet preserve optical and mechanical properties.

7. Applications

Transparent wood shows low density (approx. 1.2 g cm^{-3}), high optical transmittance (over 80%) and haze (over 70%), good mechanical performance, and potential for multi-functional modifications. Interesting application areas include smart buildings and load-bearing structures with photonic function. One may consider building applications where light transmittance can be designed so that artificial light can be partially replaced by sunlight. Li *et al.* [16] suggested that a transparent wood roof could provide more uniform and consistent illumination during the day (figure 7*a*). Compared with glass, building panels from transparent wood have lower thermal conductivity, better impact strength and lower density. The high haze with broad scattering angles is an attractive feature for solar cells [48]. Light will travel longer path lengths in the solar cell due to this light scattering phenomenon. The interaction between the light wave and the active medium is improved, so that better solar cell efficiency becomes possible. Zhu *et al.* [19] demonstrated improved solar cell efficiency of 18.02% by positioning transparent wood on top of solar cells.

Obviously, transparent wood does not show an intrinsic optical gain by itself. The addition of active optical media can therefore lead to a broader range of applications. Luminescent transparent wood [21,23] shows diffused luminescence originating from embedded QDs

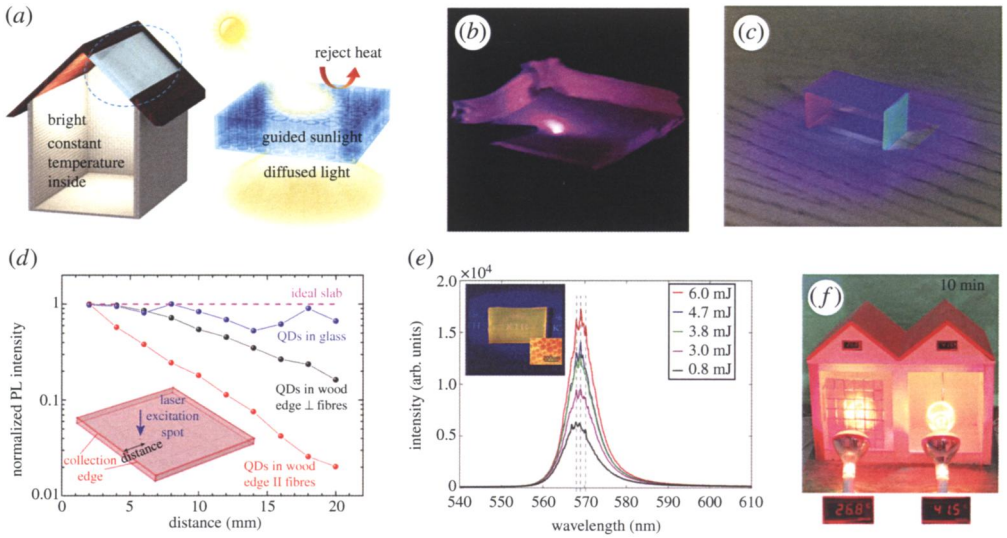

Figure 7. (*a*) A sketch of a house with a transparent wood rooftop for comfortable lighting conditions [16]. (*b*) Image of transparent wood with Si QD showing diffused luminescence [23]. (*c*) Photograph of a luminescent transparent wood stool [37]. (*d*) PL intensity for QD transparent wood as a function of excitation spot distance from the sample edge: parallel and perpendicular to the fibre direction (red and black), PL of QDs in glass collected as a reference (blue) [23]. (*e*) Evolution of fluorescence spectrum for the wood laser sample at variable pump pulse energy and fixed pump line length. The inset image is a typical dye-impregnated transparent wood sample illuminated by blue light [47]. (*f*) Image of model houses showing temperature changes after simulated solar radiation: C_{sx}WO3/transparent wood house (left) and glass house (right) after 10 min. Note temperature readings below image [20]. Reproduced with permission from Li *et al.* (Copyright © 2016 Wiley); Li *et al.* [23] (Copyright © 2017 Wiley); Li *et al.* [37] (Copyright © 2017 Wiley); Vasileva *et al.* [47] (Copyright © 2017 Wiley) and Yu *et al.* [20] (Copyright © 2017 Royal Society of Chemistry).

(figure 7*b*). This may be used in planar light sources, luminescent building elements or design furniture [23]. Li *et al*. made a luminescent transparent wood model stool by including QDs with different emission colours (figure 7*c*) [37]. The scattering pattern demonstrates the anisotropic nature of this QD transparent wood nanocomposite (figure 7*d*). The phenomenon is relevant for wood anatomy studies and wood structure imaging. With luminescent dyes, lasing emission was demonstrated [47], and wooden lasers could potentially be realized. The fibre dimensions and the size distributions influence lasing behaviour (figure 7*e*). Yu *et al*. [20] demonstrated transparent wood for heat-shielding buildings/windows by the use of NIR absorbing Cs_xWO_3 nanoparticles. Strong absorption of light was observed at wavelengths from 780 to 2500 nm. The Cs*x*WO3/transparent wood window resulted in lower temperature increase compared with the ordinary glass window reference (figure 7*f*). Transparent wood may therefore be considered for energy-saving specialty windows. Magnetic nanoparticles have also been used with transparent wood [21,22], and considered applications include magnetic switches and electromagnetic interference shielding.

For future building applications, thick and large-scale transparent wood structures are highly desirable. So far, transparent wood samples reported have been small and of low thickness. That is because with higher thickness, light undergoes longer propagation inside the transparent wood where light attenuation happens (light absorption and scattering), leading to less transmitted light. Therefore, proper polymer selection and chemical modification are vital to minimize the light attenuation. The challenge to increase thickness while managing sufficient transparency also includes the need for scalable processing concepts in order to successfully implement the technologies at large industrial scale. Efforts are needed to improve polymer infiltration for large

samples (i.e. metres large), and to minimize polymer shrinkage during polymerization. The long-term stability of optical and mechanical properties will be important for transparent wood in real applications.

8. Summary

Transparent wood was originally described in the early 1990s, with the purpose to facilitate cell structure and morphology studies of wood species. Li *et al.* then measured physical properties and outlined the possibility to use transparent wood in engineering applications [15]. This has been followed by numerous publications on various applications of the concept. New functionalization procedures in the direction of photonics applications are of great interest, including QD and organic dye additions to the material. IR-adsorbing nanoparticles have also been added to provide heat-shielding function to transparent wood. An important advantage with transparent wood is that it combines functional and structural performance so that load-bearing structures can be prepared with optical, heat-shielding or magnetic functionalities. In order to realize the vision of large-scale wood nanotechnology applications of transparent wood, nanoscale materials science needs to be developed to include scalable processing technologies for industrial implementation.

Data accessibility. This article has no additional data.

Authors' contributions. L.B. conceived the initial idea, and all authors contributed to the final design. Y.L., Q.F. and X.Y. contributed equally to the writing of this paper. All authors gave final approval for publication.

Competing interests. We declare we have no competing interests.

Funding. We acknowledge funding from KTH in the European Research Council project no. 742733, Wood NanoTech.

References

1. Eichhorn SJ *et al.* 2010 Review: current international research into cellulose nanofibres and nanocomposites. *J. Mater. Sci.* **45**, 1–33. (doi:10.1007/s10853-009-3874-0)
2. Nogi M, Iwamoto S, Nakagaito AN, Yano H. 2009 Optically transparent nanofiber paper. *Adv. Mater.* **21**, 1595–1598. (doi:10.1002/adma.200803174)
3. Rohrbach K, Li Y, Zhu H, Liu Z, Dai J, Andreasen J, Hu L. 2014 A cellulose based hydrophilic, oleophobic hydrated filter for water/oil separation. *Chem. Commun.* **50**, 13 296–13 299. (doi:10.1039/C4CC04817B)
4. Saha D, Bhattacharya S. 2010 Hydrocolloids as thickening and gelling agents in food: a critical review. *J. Food Sci. Technol.* **47**, 587–597. (doi:10.1007/s13197-010-0162-6)
5. Zhu H, Fang Z, Preston C, Li Y, Hu L. 2014 Transparent paper: fabrications, properties, and device applications. *Energy Environ. Sci.* **7**, 269–287. (doi:10.1039/C3EE43024C)
6. Moon RJ, Martini A, Nairn J, Simonsen J, Youngblood J. 2011 Cellulose nanomaterials review: structure, properties and nanocomposites. *Chem. Soc. Rev.* **40**, 3941–3994. (doi:10.1039/C0CS00108B)
7. Wang Y *et al.* 2017 A high-performance, low-tortuosity wood-carbon monolith reactor. *Adv. Mater.* **29**, 1604257. (doi:10.1002/adma.201604257)
8. Lv S, Fu F, Wang S, Huang J, Hu L. 2015 Novel wood-based all-solid-state flexible supercapacitors fabricated with a natural porous wood slice and polypyrrole. *RSC Adv.* **5**, 2813–2818. (doi:10.1039/C4RA13456G)
9. Burgert I, Cabane E, Zollfrank C, Berglund L. 2015 Bio-inspired functional wood-based materials – hybrids and replicates. *Int. Mater. Rev.* **60**, 431–450. (doi:10.1179/1743280415Y.0000000009)
10. Wang S, Lu A, Zhang L. 2016 Recent advances in regenerated cellulose materials. *Prog. Polym. Sci.* **53**, 169–206. (doi:10.1016/j.progpolymsci.2015.07.003)
11. Iwamoto S, Nakagaito ANN, Yano H, Nogi M. 2005 Optically transparent composites reinforced with plant fiber-based nanofibers. *Appl. Phys. A* **81**, 1109–1112. (doi:10.1007/s00339-005-3316-z)

12. Yano H, Sasaki S, Shams MI, Abe K, Date T. 2014 Wood pulp-based optically transparent film: a paradigm from nanofibers to nanostructured fibers. *Adv. Opt. Mater.* **2**, 231–234. (doi:10.1002/adom.201300444)
13. Taniguchi T, Okamura K. 1998 New films produced from microfibrillated natural fibres. *Polym. Int.* **47**, 291–294. (doi:10.1002/(SICI)1097-0126(199811)47:3<291::AID-PI11>3.0.CO;2-1)
14. Shams MI, Nogi M, Berglund LA, Yano H. 2012 The transparent crab: preparation and nanostructural implications for bioinspired optically transparent nanocomposites. *Soft Matter* **8**, 1369–1373. (doi:10.1039/C1SM06785K)
15. Fink S. 1992 Transparent wood—a new approach in the functional study of wood structure. *Holzforschung* **46**, 403–408. (doi:10.1515/hfsg.1992.46.5.403)
16. Li T *et al.* 2016 Wood composite as an energy efficient building material: guided sunlight transmittance and effective thermal insulation. *Adv. Energy Mater.* **6**, 1601122. (doi:10.1002/aenm.201601122)
17. Li Y, Fu Q, Yu S, Yan M, Berglund L. 2016 Optically transparent wood from a nanoporous cellulosic template: combining functional and structural performance. *Biomacromolecules* **17**, 1358–1364. (doi:10.1021/acs.biomac.6b00145)
18. Zhu M *et al.* 2016 Highly anisotropic, highly transparent wood composites. *Adv. Mater.* **28**, 5181–5187. (doi:10.1002/adma.201600427)
19. Zhu M, Li T, Davis CS, Yao Y, Dai J, Wang Y, AlQatari F, Gilman JW, Hu L. 2016 Transparent and haze wood composites for highly efficient broadband light management in solar cells. *Nano Energy* **26**, 332–339. (doi:10.1016/j.nanoen.2016.05.020)
20. Yu Z, Yao Y, Yao J, Zhang L, Zhang C, Gao Y, Luo H. 2017 Transparent wood containing CsxWO3 nanoparticles for heat-shielding-window applications. *J. Mater. Chem. A* **5**, 6019–6024. (doi:10.1039/C7TA00261K)
21. Gan W, Xiao S, Gao L, Gao R, Li J, Zhan X. 2017 Luminescent and transparent wood composites fabricated by Poly(methyl methacrylate) and γ-Fe_2O_3@YVO_4:Eu^{3+} nanoparticle impregnation. *ACS Sustain. Chem. Eng.* **5**, 3855–3862. (doi:10.1021/acssuschemeng.6b02985)
22. Gan W, Gao L, Xiao S, Zhang W, Zhan X, Li J. 2017 Transparent magnetic wood composites based on immobilizing Fe3O4 nanoparticles into a delignified wood template. *J. Mater. Sci.* **52**, 3321–3329. (doi:10.1007/s10853-016-0619-8)
23. Li Y, Yu S, Veinot JGC, Linnros J, Berglund L, Sychugov I. 2016 Luminescent transparent wood. *Adv. Opt. Mater.* **5**, 3–7. (doi:10.1002/adom.201600834)
24. Siau JF. 2012 *Transport processes in wood*. Berlin, Germany: Springer Science & Business Media.
25. Zhu H, Parvinian S, Preston C, Vaaland O, Ruan Z, Hu L. 2013 Transparent nanopaper with tailored optical properties. *Nanoscale* **5**, 3787. (doi:10.1039/c3nr00520h)
26. Peatross J, Ware M. 2011 *Physics of light and optics*. Provo, UT: Brigham Young University, Department of Physics.
27. Larena A, Millán F, Pérez G, Pinto G. 2002 Effect of surface roughness on the optical properties of multilayer polymer films. *Appl. Surf. Sci.* **187**, 339–346. (doi:10.1016/S0169-4332(01)01044-3)
28. Hsu P-C, Song AY, Catrysse PB, Liu C, Peng Y, Xie J, Fan S, Cui Y. 2016 Radiative human body cooling by nanoporous polyethylene textile. *Science* **353**, 1019–1023. (doi:10.1126/science.aaf5471)
29. Nogi M, Yano H. 2009 Optically transparent nanofiber sheets by deposition of transparent materials: a concept for a roll-to-roll processing. *Appl. Phys. Lett.* **94**, 233117. (doi:10.1063/1.3154547)
30. Emami N, Sjödahl M, Söderholm K-JM. 2005 How filler properties, filler fraction, sample thickness and light source affect light attenuation in particulate filled resin composites. *Dent. Mater.* **21**, 721–730. (doi:10.1016/j.dental.2005.01.002)
31. Müller U, Rätzsch M, Schwanninger M, Steiner M, Zöbl H. 2003 Yellowing and IR-changes of spruce wood as result of UV-irradiation. *J. Photochem. Photobiol. B* **69**, 97–105. (doi:10.1016/S1011-1344(02)00412-8)
32. Yano H. 2001 Potential strength for resin-impregnated compressed wood. *J. Mater. Sci. Lett.* **20**, 1127–1129. (doi:10.1023/A:1010996424453)
33. Yaddanapudi HS, Hickerson N, Saini S, Tiwari A. 2017 Fabrication and characterization of transparent wood for next generation smart building applications. *Vacuum* **146**, 649–654. (doi:10.1016/j.vacuum.2017.01.016)

34. Zhu M *et al.* 2017 Anisotropic, transparent films with aligned cellulose nanofibers. *Adv. Mater.* **29**, 1606284. (doi:10.1002/adma.201606284)
35. Fritz-Popovski G, Van Opdenbosch D, Zollfrank C, Aichmayer B, Paris O. 2013 Development of the fibrillar and microfibrillar structure during biomimetic mineralization of wood. *Adv. Funct. Mater.* **23**, 1265–1272. (doi:10.1002/adfm.201201675)
36. Fritz-Popovski G, Morak R, Schöberl T, Van Opdenbosch D, Zollfrank C, Paris O. 2014 Pore characteristics and mechanical properties of silica templated by wood. *Bioinspired, Biomim. Nanobiomaterials* **3**, 160–168. (doi:10.1680/bbn.14.00012)
37. Li Y, Fu Q, Rojas R, Yan M, Lawoko M, Berglund L. 2017 Lignin-retaining transparent wood. *ChemSusChem* **10**, 3445–3451. (doi:10.1002/cssc.201701089)
38. Caseri W. 2000 Nanocomposites of polymers and metals or semiconductors: historical background and optical properties. *Macromol. Rapid Commun.* **21**, 705–722. (doi:10.1002/1521-3927(20000701)21:11<705::AID-MARC705>3.0.CO;2-3)
39. Ross RJ. 2010 *Wood handbook: wood as an engineering material*, p. 1. Madison, WI: Forest Products Laboratory, General Technical Report (GTR).
40. Merk V, Chanana M, Keplinger T, Gaan S, Burgert I. 2015 Hybrid wood materials with improved fire retardance by bio-inspired mineralisation on the nano- and submicron level. *Green Chem.* **17**, 1423–1428. (doi:10.1039/C4GC01862A)
41. Trey S, Olsson RT, Ström V, Berglund L, Johansson M. 2014 Controlled deposition of magnetic particles within the 3-D template of wood: making use of the natural hierarchical structure of wood. *RSC Adv.* **4**, 35678. (doi:10.1039/C4RA04715J)
42. Gan W, Gao L, Sun Q, Jin C, Lu Y, Li J. 2015 Multifunctional wood materials with magnetic, superhydrophobic and anti-ultraviolet properties. *Appl. Surf. Sci.* **332**, 565–572. (doi:10.1016/j.apsusc.2015.01.206)
43. Guo H, Fuchs P, Cabane E, Michen B, Hagendorfer H, Romanyuk YE, Burgert I. 2016 UV-protection of wood surfaces by controlled morphology fine-tuning of ZnO nanostructures. *Holzforschung* **70**, 699–708. (doi:10.1515/hf-2015-0185)
44. Chen C *et al.* 2017 All-wood, low tortuosity, aqueous, biodegradable supercapacitors with ultra-high capacitance. *Energy Environ. Sci.* **10**, 538–545. (doi:10.1039/C6EE03716J)
45. Zhang Y *et al.* 2017 High-capacity, low-tortuosity, and channel-guided lithium metal anode. *Proc. Natl Acad. Sci.* **114**, 3584–3589. (doi:10.1073/pnas.1618871114)
46. Material SC. 2014 A study on the morphology, mechanical, and electrical performance of polyaniline-modified wood—a semiconducting composite material. *BioResource* **9**, 5007–5023.
47. Vasileva E, Li Y, Sychugov I, Mensi M, Berglund L, Popov S. 2017 Lasing from organic dye molecules embedded in transparent wood. *Adv. Opt. Mater.* **5**, 1700057. (doi:10.1002/adom.201700057)
48. Fang Z *et al.* 2014 Novel nanostructured paper with ultrahigh transparency and ultrahigh haze for solar cells. *Nano Lett.* **14**, 765–773. (doi:10.1021/nl404101p)